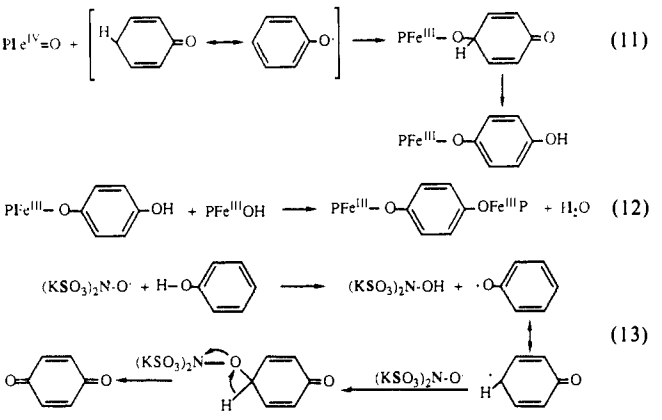

proposed in reaction 11. In related work, Seok and Meyer[42] have shown that complexes containing the Ru^{IV}=O group are capable of oxidizing phenols to quinones. It is unlikely that the *p*-hydroquinone derived complexes arise from the reaction of the phenoxy radical with dioxygen. It is known that the reactivity of phenoxy radicals, like phenyl radicals, toward dioxygen is low[37] and that radical/radical coupling is favored over reaction with dioxygen.[43]

Peroxidases are known to catalyze oxidations of phenols.[44-46] However, our current picture of the heme cavity in the horseradish peroxidase seems to preclude, in most cases, direct interaction of ferryl states with substrates whose entry to the heme pocket is restricted.[47] Thus, these enzymatic oxidations are likely to involve reactions fundamentally different than those studied here where the phenoxy radical is generated in the immediate vicinity of the iron porphyrin.

Experimental Section

Materials. Samples of $TTPFe^{III}(Ar)$ were prepared from $TTPFe^{III}Cl$ and the appropriate Grignard reagent by an established procedure[11-13] and handled in a dioxygen-free glovebox. Samples of $TTPFe^{III}(OAr)$ were prepared by addition of an excess of the solid sodium salt of the phenolate to $TTPFe^{III}Cl$ in toluene or chloroform solution, sonication of the mixture, and filtration to remove the sodium phenolate and sodium chloride. Toluene-d_8, chloroform-*d*, and dichloromethane-d_2 were deoxygenated and stored in a dinitrogen-filled glovebox before use.

Oxygenation Experiments. A 3 mM solution of $TTPFe^{III}(Ar)$ in toluene-d_8, chloroform-*d*, or dichloromethane-d_2 was prepared under a dinitrogen atmosphere, placed in a 5-mm NMR tube, sealed with a rubber septum cap, and wrapped with Parafilm. Dioxygen was admitted to the sample through a microliter syringe while controlling the temperature of the sample. The sample was shaken to facilitate dioxygen uptake and placed in the NMR spectrometer for spectral observation.

Instrumentation. NMR spectra were recorded on Nicolet NT-360 FT and NT-500 FT spectrometers operating in the quadrature mode (^1H frequencies are 360 and 500 MHz, respectively). The spectra were collected over a 40-kHz bandwidth with 16 K data points and a 6-μs 90° pulse. For a typical paramagnetic spectrum, between 500 and 2000 transients were accumulated with a delay time of 50 ms. The signal-to-noise ratio was improved by apodization of the free induction decay. The residual methyl peak of toluene was used as a secondary reference, which was set at 2.09 ppm. To obtain line widths of overlapping resonances, the spectra were deconvoluted by using the NTC CAP routine of the Nicolet software. ESR spectra were recorded on a Bruker spectrometer at X band.

Acknowledgment. We thank the National Institutes of Health (Grant GM-26226) for support.

(39) Waters, W. A. *Mechanisms of Oxidation of Organic Compounds*; Methnen and Co.: London, 1964; p 147.
(40) Teuber, H. J.; Dietz, K. H. *Angew. Chem., Int. Ed. Engl.* **1965**, *4*, 871.
(41) Zimmer, H.; Lankin, D. C.; Horgan, S. W. *Chem. Rev.* **1971**, *71*, 229.
(42) Seok, W. K.; Meyer, T. J. *J. Am. Chem. Soc.* **1988**, *110*, 7358.
(43) Blanchard, H. S. *J. Org. Chem.* **1960**, *25*, 264.
(44) Hewson, W. D.; Dunford, H. B. *J. Biol. Chem.* **1976**, *251*, 6043.
(45) Shiga, T.; Imaizumi, K. *Arch. Biochem. Biophys.* **1975**, *167*, 469.
(46) Buhler, D. R.; Mason, H. S. *Arch. Biochem. Biophys.* **1961**, *92*, 424.
(47) Ortiz de Montellano, P. R. *Acc. Chem. Res.* **1987**, *20*, 289.

Production and Storage of Multiple, Photochemical Redox Equivalents on a Soluble Polymer

Laura A. Worl,[1a] Geoffrey F. Strouse, Janet N. Younathan,[1b] Steven M. Baxter, and Thomas J. Meyer*

Contribution from the Department of Chemistry, University of North Carolina, Chapel Hill, North Carolina 27599. *Received December 18, 1989*

Abstract: Soluble polymers have been prepared that contain high loadings of metal-to-ligand charge-transfer (MLCT) visible-light absorbers based on polypyridyl complexes of Ru^{II} or Os^{II}. The complexes have been attached to a styrene/chloromethylstyrene copolymer by nucleophilic displacement of the chloro groups. By using excesses of the complexes, complete substitution at the available ~30 chloro-methylated sites was achieved. A series of mixed-valence polymers with controlled M^{III}/M^{II} ratios has been prepared in acetonitrile or acidic aqueous solution by oxidation with Ce(IV). For the Os^{II}-containing polymers, Os^{II}*-based MLCT excited-state lifetimes and emission quantum yields are relatively unaffected by the Os^{III}/Os^{II} ratio. This shows that intramolecular oxidative quenching of Os^{II}* by Os^{III} is slow. The slow rate of electron-transfer quenching is a manifestation of the "inverted region". Because excited-state properties are relatively unaffected in the mixed-valence polymers, it is possible to build up and store ~30 oxidative equivalents on individual polymeric strands by photochemical oxidation.

Introduction

In molecular systems, well-defined processes exist in which single photon excitation leads to the production of redox equivalents with relatively high efficiency,[2,3] e.g., eq 1 where PQ^{2+} =

$$Ru(bpy)_3^{2+} \xrightarrow{h\nu} Ru(bpy)_3^{2+*} \quad (1a)$$

$$Ru(bpy)_3^{2+*} + PTZ \rightarrow Ru(bpy)_3^{+} + PTZ^{+} \quad (1b)$$

$$Ru(bpy)_3^{2+*} + PQ^{2+} \rightarrow Ru(bpy)_3^{3+} + PQ^{+} \quad (1c)$$

(1) (a) Current address: Los Alamos National Labs, Los Alamos, NM 87545. (b) Current address: Eastman Kodak Company, Rochester, NY 14650.

0002-7863/90/1512-7571$02.50/0

N,N'-methyl-4,4'-bipyridinium dication and PTZ = phenothiazine. These processes are based on single electron transfer events, which necessarily limits the number of redox equivalents produced per photon to 1. In potential applictions involving the utilization of light energy for the production of chemical products such as the photochemical splitting of water, eq 2, the component half-reactions are inherently multielectron in character.

$$2H_2O \rightarrow O_2 + 2H_2 \quad (2)$$

$$2H_2O \rightarrow O_2 + 4e^- + 4H^+ \quad (3a)$$

$$4H^+ + 4e^- \rightarrow 2H_2 \quad (3b)$$

A problem exists in discrete molecular systems in finding ways to couple single photonic excitation to the multielectron requirements of small molecule reactions. The difficulties arise from the mechanistic demands of the reactions. For example, in either water oxidation or reduction, single one-electron transfers produce high-energy intermediates such as $^{\bullet}OH$ or $H^{\bullet}$.

In photosynthesis the energy transduction mechanism between single photonic events and water oxidation involoves a sequence of single photochemical electron transfers followed by delivery and storage of multiple redox equivalents at a catalytic site for water oxidation.[4] The oxygen-evolving site is thought to be based on a Mn cluster at which the oxidation of water to O_2 occurs.[5]

One approach to assembling these characteristics in artificial systems is to utilize the excited-state electron-transfer properties of metal complexes that are bound to polymers. On the basis of known polymer chemistry, there are a number of approaches available for assembling multiple components on single, polymeric strands. For example, soluble polymers containing the Ru–bpy chromophore have been prepared.[6-12] In one synthetic approach, intact complexes were added to a preformed styrene/chloromethylstyrene backbone by the nucleophilic displacement of chloride.[8] In these polymers it has been shown that light-induced electron-transfer chemistry in solution is retained at the metal complex sites. These polymers were subsequently exploited in a complicated scheme in which quenching and subsequent electron transfer led to the storage of oxidative or reductive equivalents on separate polymeric strands.[8b]

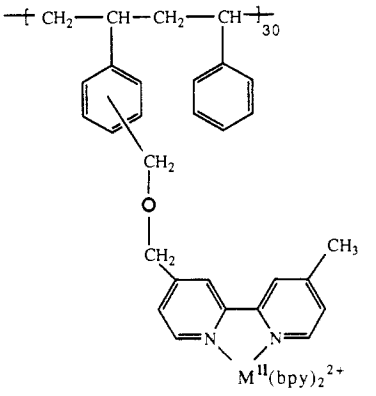

M = Ru: $[PS\text{-}Ru^{II}_{30}](PF_6)_{60}$

Os: $[PS\text{-}Os^{II}_{30}](PF_6)_{60}$

Figure 1. Structures of the Ru^{II} and Os^{II} redox polymers.

We have exploited the anionic displacement chemistry in the preparation of related polymers. In one type of material the extent of loading of Ru^{II} or Os^{II} metal complexes per available chloromethylated site was complete with, on the average, ~30 sites bound/30 sites available (Figure 1). One of our goals was to use these polymers to mimic the ability of the photosynthetic system to produce and store multiple redox equivalents.

The scheme that we envisaged involved the use of a sequence of one-photon, one-electron photochemical steps. An example is shown in eq 4 where M = Ru or Os and Ox/Red is an external redox couple. The relationship between the abbreviation used for the polymer and its repeating structure is shown in Figure 1.

$$\xrightarrow{h\nu} [PS\text{-}M^{II}{}^{*}M^{II}_{29}]^{60+} + Ox \rightarrow [PS\text{-}M^{III}M^{II}_{29}]^{61+} + Red$$

$$\xrightarrow{h\nu} [PS\text{-}M^{III}M^{II}{}^{*}M^{II}_{28}]^{61} + Ox \rightarrow [PS\text{-}M^{III}{}_2M^{II}_{28}]^{62+} + Red \quad (4)$$

$$\vdots$$

$$\xrightarrow{h\nu} [PS\text{-}M^{II}{}^{*}M^{III}_{29}]^{89+} + Ox \rightarrow [PS\text{-}M^{III}{}_{30}]^{90+} + Red$$

Following optical excitation of a partly oxidized polymer, the excited-state ($M^{II}{}^{*}$) and oxidized (M^{III}) sites are scattered randomly along individual polymeric strands. The M^{III} sites are relatively strong oxidants, readily capable of quenching $M^{II}{}^{*}$. Because of the coexistence of excited-state and quencher sites on individual polymeric strands, an inherent limitation in such schemes arises from intramolecular electron-transfer quenching, e.g., eq 5, which is highly favored thermodynamically. Mecha-

$$[PS\text{-}Ru^{III}Ru^{II}{}^{*}Ru^{II}_{28}]^{61+} \rightarrow [PS\text{-}Ru^{II}Ru^{III}Ru^{II}_{28}]^{61+} \quad (5)$$
$$\Delta G^{\circ\prime} = -2.1 \text{ eV}$$

nisms exist for bringing the oxidative quencher and the excited state to adjacent sites. One is by intramolecular electron transfer between M^{II} and M^{III}, eq 6a, which is expected to be rapid.[2d,13,14]

(2) (a) Juris, A.; Balzani, V.; Barigelletti, F.; Campagna, S.; Belser, P.; Von Zelewsky, A. *Coord. Chem. Rev.* **1988**, *84*, 85. (b) *Energy Resources through Photochemistry and Catalysis*; Grätzel, M., Ed.; Academic Press: New York, 1983. (c) Meyer, T. J. *Acc. Chem. Res.* **1989**, *22*, 163. (d) Sutin, N.; Creutz, C. *Pure Appl. Chem.* **1980**, *52*, 2717. (e) Kalyanasundaram, K. *Coord. Chem. Rev.* **1982**, *46*, 159. (f) Whitten, D. G. *Acc. Chem. Res.* **1980**, *13*, 83.

(3) (a) Maestri, M.; Grätzel, M. *Berichte der Bunsen-Gesellsch.* **1977**, *81*, 504. (b) Bock, C. R.; Meyer, T. J.; Whitten, D. G. *J. Am. Chem. Soc.* **1974**, *96*, 4710. (c) Gafney, H. D.; Adamson, A. W. *J. Am. Chem. Soc.* **1972**, *94*, 8238.

(4) (a) Clayton, R. K. *Photosynthesis: Physical Mechanism and Chemical Patterns*; Cambridge University Press: London, 1980. (b) Barber, J. *Photosynthesis in Relation to Model Systems*; Elsevier: New York, 1979.

(5) Brudvig, G. N. *J. Bioenerg. Biomembr.* **1987**, *19*, 91.

(6) (a) *Polymer Photophysics*; Phillips, D., Ed.; Chapman and Hall: New York, 1985. (b) Guillet, J. *Polymer Photophysics and Photochemistry*; Cambridge University Press: New York, Chapter 9. (c) Webber, S. E. In *New Trends in the Photochemistry of Polymers*; Allen, N. S., Rabek, J. E., Eds.; Elsevier: New York, 1985.

(7) (a) Sassoon, R. E.; Rabani, J. *J. Phys. Chem.* **1985**, *89*, 5500. (b) Rabani, J.; Sasson, R. E. *J. Photochem.* **1985**, *29*, 7.

(8) (a) Margerum, L. D.; Murray, R. W.; Meyer, T. J. *J. Phys. Chem.* **1986**, *90*, 7289. (b) Olmsted, J., III; McClanahan, S. F.; Danielson, E.; Younathan, J. N.; Meyer, T. J. *J. Am. Chem. Soc.* **1987**, *109*, 3297. (c) Younathan, J. N.; McClanahan, S. F.; Meyer, T. J. *Macromolecules* **1989**, *22*, 1048. (d) Margerum, L. D.; Murray, R. W.; Meyer, T. J. *J. Phys. Chem.* **1986**, *90*, 2696.

(9) (a) Furue, M.; Kuroda, N.; Sano, S. *J. Macromol. Sci.-Chem.* **1988**, *A25*, 1263. (b) Sumi, K.; Furue, M.; Nozakura, S.-I. *J. Polym. Sci., Polym, Chem. Ed.* **1985**, *23*, 3059. (c) Sumi, K.; Furue, M.; Nozakura, S. *Photochem. Photobiol.* **1985**, *42*, 485. (d) Furue, M.; Sumi, K.; Nozakura, S. *Chem. Lett.* **1981**, 1349.

(10) (a) Kaneko, M.; Nakamura, H. *Macromolecules* **1987**, *20*, 2265. (b) Hou, X.-H.; Kaneko, M.; Yamada, A. *J. Polym. Sci., Polym, Chem. Ed.* **1986**, *24*, 2749. (c) Kaneko, M.; Yamada, A.; Tsuchida, F.; Kurimura, Y. *J. Phys. Chem.* **1984**, *88*, 1061. (d) Kurimura, Y.; Shinozaki, M.; Ito, F.; Uratani, Y.; Shigehara, K.; Tsuchida, E.; Kaneko, M.; Yamada, A. *Bull. Chem. Soc. Jpn.* **1982**, *55*, 380.

(11) (a) Ennis, P. M.; Kelly, J. M. *J. Phys. Chem.* **1989**, *93*, 5735. (b) Ennis, P. M.; Kelly, J. M.; O'Connell, C. M. *J. Chem. Soc., Dalton Trans.* **1986**, 2485. (c) Kelly, J. M.; Long, C.; O'Connell, C. M.; Vos, J. G.; Tinnemans, A. H. A. *Inorg. Chem.* **1983**, *22*, 2818.

(12) (a) Ghiggino, K. P.; Brown, J. M.; Launikonis, A.; Mau, A. W.-H.; Sasse, W. H. F. *Aust. J. Chem.* **1988**, *41*, 9. (b) Degani, Y.; Heller, A. *J. Am. Chem. Soc.* **1989**, *111*, 2357. (c) Nakahira, T.; Inoue, Y.; Iwasaki, K.; Tanigawa, H.; Kouda, Y.; Iwabuchi, S.; Kojima, K. *Makromol. Chem., Rapid Commun.* **1988**, *9*, 13.

(13) (a) Yang, E. S.; Chan, M.-S.; Wahl, A. C. *J. Phys. Chem.* **1975**, *79*, 2049. (b) Meyer, T. J.; Taube, H. In *Comprehensive Coordination Chemistry, The Synthesis, Reactions, Properties, & Applications of Coordination Compounds*; Wilkinson, G. S., Ed.; Pergamon Press: Oxford, 1987; Vol. 1, p 331. (c) Young, R. C.; Keene, R. F.; Meyer, T. J. *J. Am. Chem. Soc.* **1977**, *99*, 2468.

A second is by intramolecular energy transfer, eq 6b.

$$\sim Ru^{III}Ru^{II}Ru^{II*}\sim \rightarrow \sim Ru^{II}Ru^{III}Ru^{II*}\sim \quad (6a)$$

$$\sim Ru^{III}Ru^{II}Ru^{II*} \rightarrow \sim Ru^{III}Ru^{II*}Ru^{II}\sim \quad (6b)$$

With the existence of facile intramolecular energy or electron transfer on individual strands, the quenching of M^{II*} by M^{III} could be of importance even in the initial stages of eq 4 when the number of M^{III} quenching sites is low. This quenching would greatly impair the ability of the polymers to accumulate multiple redox equivalents.

There is experimental evidence in related reactions that indicates that electron transfer can be slow if ΔG is large and negative.[15,16] At first glance, this is a surprising result since these reactions, for example, the oxidative quenching of $[Ru(bpy)_3]^{2+*}$ by $[Ru(bpy)_3]^{3+}$,[15] are highly favored thermodynamically. Slow electron transfer *is* consistent with theoretical predictions concerning electron transfer in the "inverted" region.[17] In this region, electron transfer rate constants are predicted to *decrease* as $-\Delta G$ increases. The decrease is a natural consequence of the large energy release that occurs in the quenching step. Electron transfer in the inverted region shares with the nonradiative decay of excited states certain common features. The dynamics of either are dictated, in part, by the dissipation of the initial electronic energy into intramolecular vibrations and the librational modes of the solvent.[18]

We show here that the constraints to electron transfer that are predicted to exist in the inverted region appear in soluble polymers that are fully loaded with polypyridyl chromophores. Because of the inverted region, quenching of M^{II*} excited states on individual polymeric strands by M^{III} is *not* an important process. Because of the absence of intramolecular quenching, it is possible to create and store multiple redox equivalents on individual polymeric strands with relatively high, per-photon-absorbed quantum efficiencies.

Experimental Section

General Considerations. Dimethyl sulfoxide (DMSO) was stirred over potassium hydroxide, distilled under reduced pressure, and stored under Ar. Tetrahydrofuran (THF) was heated at reflux over potassium metal and distilled immediately prior to use. Sephadex LH-20 (25–100 μm bead size) for column chromatography was supplied by Sigma Chemical Co. and was swollen in the eluting solvent prior to separation. Ammonium cerium(IV) nitrate, $(NH_4)Ce(NO_3)_6$, was received from Aldrich.

For excited-state measurements, spectroscopic grade acetonitrile (CH_3CN) was used as received from Burdick and Jackson and stored over molecular sieves. For emission and lifetime data, dilute solutions (10^{-5}–10^{-4} M) of the complexes were freeze–pump–thaw degassed at $<10^{-5}$ Torr for a minimum of five cycles and sealed under vacuum in 9-mm glass cells or bubble deoxygenated with argon for a minimum of 30 min. All samples were protected from exposure to light prior to measurements.

The salt 4-methoxybenzenediazonium tetrafluoroborate ($[4\text{-}CH_3OC_6H_4N_2](PF_6)$, Aldrich) was used as received and stored in the dark at 0 °C. Phenothiazine (PTZ, Alfa) was recrystallized twice from toluene; methylene viologen (PQ^{2+}) as the Cl^- salt was converted into the PF_6^- salt after being received from Aldrich. Both reagents were stored in a desiccator and protected from light.

Infrared spectra were recorded in solution on a Nicolet 20DX FTIR spectrometer and were corrected for the solvent background. NMR analyses were carried out on a Bruker AC200 instrument in CD_3CN. Gel permeation chromatography was carried out in THF by using an IBM LC/9560 solvent delivery system equipped with a LC/9525 differential refractometer detector and styrene–divinylbenzene column types A, C, and E (IBM) connected in order of decreasing pore size. Molecular weights were established by using polystyrene standards.

Molecular Modeling. In an effort to establish the morphology and spatial arrangement of the metal complexes on the polymers, a molecular mechanics analysis was performed. The force field employed contained potential terms for bonding stretching, bending, torsion, non-bonded interactions, and coulombic repulsion.[32,35]

Measurements. Absorption spectra were obtained by using a Hewlett Packard 8415A diode array spectrophotometer. The measurements were made versus a solvent blank by using matched 1-cm quartz cells. Solutions of Ce^{IV} in CH_3CN were prepared and standardized as described previously.[19] The solutions were prepared immediately before use because of their instability over a period of ~12 h. Titrations involving Ce^{IV} were carried out by adding known aliquots of oxidant to solutions of the complex and monitoring the changes in absorbance. To establish the reaction stoichiometry, plots of absorbance at a particular wavelength (normally λ_{max}) were made versus the moles of oxidant added/moles of complex.

Spectroelectrochemical experiments were carried out under argon by using an all-quartz three-compartment cell. Electrochemical data were obtained by cyclic voltammetry by using a Princeton Applied Research 173 potentiostat and a triangular waveform generator with the output plotted on a Hewlett-Packard 7015B XY recorder. A platinum bead working electrode, a platinum wire auxiliary electrode, and a saturated sodium chloride calomel electrode (SSCE) were used in a single compartment cell design. Solutions containing the complexes at 10^{-3} M were prepared in dry degassed acetonitrile with 0.1 M supporting electrolyte present, either tetraethylammonium perchlorate (TEAP) or tetra-*n*-butylammonium hexafluorophosphate (TBAH). Electrolysis and coulometric experiments, were performed in a three-compartment cell in which the working electrode was a Pt gauze electrode potentiostated at +1.3 V in ca. 10 mL of a 1 N H_2SO_4 solution containing $\sim 1 \times 10^{-3}$ M $[PS\text{-}Ru^{II}_{30}](PF_6)_{60}$. The electrolysis was monitored by spectrophotometric measurements as well. Qualitative measurements of chlorine production were made by sweeping the chlorine from the reaction vessel by an argon purge into a cold, aqueous basic solution. Chlorine was determined as hypochlorite by standard iodometric titration techniques.[20]

Excited-State Measurements. Corrected steady-state emission spectra were recorded and quantum yields were determined by using a SPEX F212 photoncounting spectrofluorimeter interfaced with a DM1B computer. Emission lifetimes were obtained by using the 337-nm fundamental of a Photochemical Research Associates, Inc. (PRA) LN1000 nitrogen laser as a pulsed excitation source (pulse width of 3 ns at 50 μJ/pulse) in conjunction with a ISA H-20 0.20-m tunable dye laser with dyes Coumarin 460 or 530. A dichromate solution filter was placed before the monochromator to remove scattered laser light. Emission decay was monitored at right angles by using a ISA H-20 0.20-m monochromator, a Hamamatsu R928 waater-cooled PMT, and a Tektronix 7912 or a LeCroy 6880/6010 transient digitizer interfaced to an IBM PC. Lifetimes were analyzed by either single or bi-exponential fitting routines based on the Marquardt method of analysis for nonlinear weighted least-squares fitting to the desired function.[21] The quality of the fits was determined by plotting simple residuals or weighted residuals versus time and judging the random distribution of the deviance in the plots.

Relative emission quantum yields at room temperature were determined by integrating emission spectra obtained in degassed, optically dilute (OD < 0.1) CH_3CN solutions. Absolute yields were calculated by comparisons with the standards $[Ru(bpy)_3](PF_6)_2$ for the Ru samples and $[Os(bpy)_3](PF_6)_2$ for the Os samples by using techniques described elsewhere.[22,23]

Steady-state photolyses were performed on 4.00-mL samples $\sim 10^{-4}$ in polymer in 1 M $[N(n\text{-}C_4H_9)]_4(PF_6)$–$CH_3CN$ solution with a 10-fold excess of $[4\text{-}CH_3OC_6H_4N_2](PF_6)$ added. The solution was bubble deoxygenated for 30 min. The photolysis apparatus was a SPEX housed Osram 450 W Xe lamp with excitation at 460 nm. The input photonic

(14) (a) Meyer, T. J. In *Mechanistic Aspects of Inorganic Reactions, ACS Symposium Series 198*; Rorabacher, D. B., Endicott, J. F., Eds.; American Chemical Society: Washington, 1982; p 137. (b) Meyer, T. J. In *Mixed-Valence Compounds*; Brown, D. B., Ed.; D. Reidel: Dordrecht, 1980; NATO Advanced Study Institute Series, No. 58. (c) Bignozzi, C. A.; Roffia, S.; Scandola, F. *J. Am. Chem. Soc.* **1985**, *107*, 1644.

(15) Creutz, C.; Chou, M.; Netzel, T. L.; Okumara, M.; Sutin, N. *J. Am. Chem. Soc.* **1980**, *102*, 1309.

(16) (a) Schanze, K. S.; Neyhart, G. A.; Meyer, T. J. *J. Phys. Chem.* **1986**, *90*, 2182. (b) Schanze, K. S.; Meyer, T. J. *Inorg. Chem.* **1985**, *24*, 2123.

(17) (a) Marcus, R. A. *Discuss. Faraday Soc.* **1960**, *29*, 21. (b) Marcus, R. A. *J. Chem. Phys.* **1965**, *43*, 1261.

(18) (a) Englman, R.; Jortner, J. *Mol. Phys.* **1970**, *18*, 145. (b) Freed, K. F.; Jortner, J. *J. Chem. Phys.* **1970**, *52*, 6272. (c) Jortner, J. *J. Chem. Phys.* **1976**, *64*, 4860. (d) Kober, E. M.; Caspar, J. V.; Lumpkin, R. S.; Meyer, T. J. *J. Phys. Chem.* **1986**, *90*, 3722. (c) Chen, P.; Duesing, R.; Tapolsky, G.; Meyer, T. J. *J. Am. Chem. Soc.* **1989**, *111*, 8305.

(19) (a) Prabhakar, G.; Murthy, A. R. V. A. *Anal. Chem.* **1961**, *180*, 169. (b) Callahan, R. W. Ph.D. Dissertation, Chapel Hill, NC, 1975.

(20) (a) Skoog, D. A.; West, D. M. *Fundamentals of Analytical Chemistry*; Saunders College Publishing: Philadelphia, **1982**; Chapter 15, p 31. (b) Ellis, C. D.; Gilbert, J. A.; Murphy, R.; Meyer, T. J. *J. Am. Chem. Soc.* **1983**, *105*, 4842.

(21) Instrumental interfacing and data analysis programs were written by E. Danielson.

(22) (a) Caspar, J. V.; Kober, E. M.; Sullivan, B. P.; Meyer, T. J. *J. Am. Chem. Soc.* **1982**, *104*, 630. (b) Kober, E. M.; Caspar, J. V.; Lumpkin, R. S.; Meyer, T. J. *J. Phys. Chem.* **1986**, *90*, 3722.

(23) Parker, C. A.; Rees, W. T. *Analyst (London)* **1960**, *85*, 587.

Table I. Properties of $[PS\text{-}Ru^{II}_{30}](PF_6)_{60}$ and $[PS\text{-}Os^{II}_{30}](PF_6)_{60}$ at 295 ± 2 K in CH_3CN

compd	$\lambda_{max,abs}$,[a] nm (ϵ, 10^{-4} M^{-1} cm^{-1})	$E_{1/2}$,[b] V M(III/II)	$\lambda_{max,em}$,[c] nm	ϕ_{em}[d]	τ,[d] ns
$[PS\text{-}Ru^{II}_{30}](PF_6)_{60}$	456 (1.34)	1.26	635	0.059	994[e]
$[Ru(bpy)_2(bpy\text{-}CH_2OH)](PF_6)_2$	456 (1.34)	1.24	637	0.061	1036
$[PS\text{-}Os^{II}_{30}](PF_6)_{60}$	460 (1.20), 486 (1.29)	0.75	765	0.0019	46
$[Os(bpy)_2(bpy\text{-}CH_2OH)](PF_6)_2$	460 (1.2), 485 (1.3)	0.73	760	0.0030	45

[a] For the lowest energy, intense absorption feature in the spectrum, ±2 nm. [b] The estimated error is ±0.01 V for the M(III/II) couples. Potentials for the reductive couples involving the polypyridyl ligands are not reported due to overlapping styrene reductions. [c] Corrected emission maximum, ±3 nm. [d] ±5% in ϕ_{em}; ±2% in τ. [e] From a single exponential fit of the long-lived decay component, see text.

density under the experimental conditions used was determined by actinometry with potassium ferrioxalate[24] to be 1.80×10^{-6} quanta/(s dm^{-3}). The rate of photolysis in a stirred solution was monitored by observing the fall in emission intensity at an angle of 90° to the excitation beam either at 740 nm for Os^{II} or 630 nm for Ru^{II}.

Synthesis. The modified polystyrene samples were stored in a desiccator and protected from light. The salts, $[Ru^{II}(bpy)_2(bpy\text{-}CH_2OH)](PF_6)_2$ and $[Os^{II}(bpy)_2(bpy\text{-}CH_2OH)](PF_6)_2$(bpy-$CH_2OH$ is 4-(hydroxymethyl)-4′-methyl-2,2′-bipyridine) were prepared as described previ-

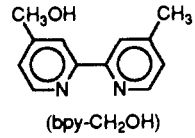

(bpy-CH_2OH)

ously.[25] The 1:1 copolymer poly(*m,p*-chloromethylstyrene-*stat*-styrene), $[PS\text{-}CH_2Cl]_{30}$, was prepared by a literature procedure.[25,26] For this polymeric sample the polydispersity, defined as the ratio of the number average molecular weight (M_n) to the weight average molecular weight (M_w), was $M_n/M_w \sim 2.30$. The *meta* to *para* distribution of the chloromethyl groups was 60:40. The free radical procedure used in the preparation is known to give atactic samples.[26] Upon addition of the complex, the resulting polymer loses its solubility in nonpolar solvents and begins to adopt the solubility characteristics of the component metal complex salts. The chemically modified polymers were reasonably soluble in CH_3CN, CH_2Cl_2, and DCE but lost solubility due to decomposition if exposed to temperatures in excess of 70 °C for periods in excess of 24 h.

Preparation of the M(II) (M = Ru, Os) Containing Polymers. The polymer salts, $[PS\text{-}M^{II}_{30}](PF_6)_{60}$ (M = Ru, Os) were prepared by stirring a solution containing the appropriate salt $[M^{II}(bpy)_2(bpy\text{-}CH_2OH)](PF_6)_2$ (1.2 equiv per CH_2Cl) and $[PS\text{-}CH_2Cl]_{30}$ at room temperature under Ar for 18 h in DMSO at (5 mL) containing 4 equiv of powdered CsOH. The crude reaction mixture was chromatographed on a 3-in. column of Sephadex LH-20 (acetone), dried in vacuo, and purified without further workup on a 3-in. column of Sephadex LH-20 (CH_3CN) to yield for M = Ru a deep black-red solid. Anal. Calcd for 100 mol % loading: C, 52.36; H, 3.92; N, 7.48; Cl, 0.00. Found: C, 52.61; H, 4.00; N, 7.02; Cl, <0.1. For M = Os a black-green solid was obtained. Anal. Calcd for 100 mol % loading: C, 48.52; H, 3.66; N, 6.93; Cl, 0.00. Found: C, 49.10; H, 4.00; N, 7.28; Cl, <0.03.

^1H NMR Analysis. The compositions of the chemically modified polymers with regard to their metal complex content were established by ^1H NMR. Only minor perturbations in the spectra of the monomers $[M(bpy)_2(bpy\text{-}CH_2OH)]^{2+}$ (M = Ru, Os) were observed upon attachment to the polymer.[8c] Attachment caused an upfield shift in the position of the bpy-CH_2O resonance such that it became coincident with the PhCH_2 resonance of the backbone at 4.6 ppm. This obviated the use of these peaks as a direct measure of polymer loading. The resonances due to the 6,6′-bipyridine protons (8.5 ppm) and the 4′-CH_3 protons on the functionalized bipyridine (2.5 ppm) appear in regions that are free from interfering signals from the backbone. Integration of these peaks versus those in an appropriate backbone region (6.2 to 6.6 ppm) provided a quantitative measure of the extent of polymer loading. On the basis of these integrations, it was shown that the ratio of complex to repeating *stat-m,p*-chloromethylstyrene–styrene unit was 1:1 to within ±10%, consistent with the average unit formula $[PS\text{-}M^{II}_{30}](PF_6)_{60}$.

Results

The polymer systems studied here contained high loadings of the Ru^{II} or Os^{II} polypyridyl complexes on single polymeric strands. The structures of the metal complex containing units in the repeating array were illustrated in Figure 1. In Table I are summarized the ground- and excited-state properties of the polymers and of their respective monomers.

Chemical Generation of the Mixed-Valence Polymers in Solution. The oxidized polymers that contain Ru^{III} are highly oxidizing (Table I). We initially attempted to work with $[PS\text{-}Ru^{II}_{30}](PF_6)_{60}$ and its oxidized forms $PS\text{-}[Ru^{III}_nRu^{II}_{(30-n)}]^{(60+n)+}$ in solution. The oxidized forms were generated electrochemically or chemically by using Ce^{IV} in 1 M H_2SO_4 solution. Under these conditions, the multiply oxidized polymers are inherently unstable both toward self-oxidation and toward oxidation of added Cl^-, At $[Cl^-] = 1 \times 10^{-3}$ M in ~1.5 N H_2SO_4, the Ru^{III} sites on the polymer return to Ru^{II} with $t_{1/2}$ ~3 min as shown by the increase in absorbance (460 nm) and emission (640 nm) intensities in the solution. Chlorine was shown to be the product of oxidation by collecting the gas above the reaction mixture; no O_2 evolution was observed. Even in the absence of Cl^-, the Ru^{III} sites in the polymer return to Ru^{II} and at a noticeably faster rate ($t_{1/2} \sim 8$ min) than $[Ru(bpy)_3]^{2+}$ under the same conditions. There was no sign of O_2 evolution in the absence of Cl^-.[27] The origin of the instability arises in self-oxidation. Oxidative electrolysis at a Pt-gauze electrode at 1.3 V in 0.1 M $[N(n\text{-}C_4H_9)]_4(PF_6)/CH_3CN$ occurred well past $n = 1$ per Ru^{II}. In the oxidized material a new absorption band appears at 241 nm, which is characteristic of the acetophenone carbonyl end groups in oxidized polystyrene.[28-30] Solution IR spectra show strong bands at 2019 and 1711 cm^{-1} after electrochemical oxidation, the latter being consistent with ν(CO) of a ketone group. Although we have not attempted to explore the point in detail, it appears that self-oxidation involves ketone formation in the polystyrene backbone, perhaps via reaction 7.

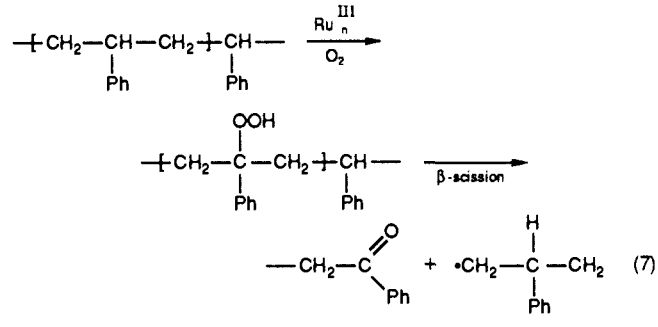

This is a reasonable suggestion given the known photooxidation of polystyrene itself which is thought to occur via the radical –C(O•)Ph– to give the ketone (ν(CO) = 1690 cm^{-1}).[29,30] Deronizer has shown that a Ru^{II} polypyridyl complex in solution can ef-

(24) Calvert, J. G.; Pitts, J. N. *Photochemistry*; John Wiley & Sons, Inc.: New York, 1966; Chapter 7.
(25) Youanthan, J. N.; McClanahan, S. F.; Meyer, T. J. *Macromolecules* **1989**, *22*, 1048.
(26) Arshady, R.; Reddy, B. S. R.; George, M. H. *Polymer* **1984**, *25*, 716.
(27) Measurements of dioxygen in the gas phase were attempted by using a Hewlett-Packard Model 5890 gas chromatograph equipped with a 5-Å molecular sieve column. The column temperature was 90 °C, and the helium gas flow rate was 30 mL/min. Samples (20 μL) were syringed from the two-compartment airtight cell, and the quantities of O_2 obtained were calculated on the basis of the known 6-mL volume dead space above the cell. From these results, the O_2 that was present after complete return of Ru^{III} to Ru^{II} was not noticeably different from the background.
(28) Wandelt, B. *Eur. Polym. J.* **1986**, *22*, 755.
(29) Geuskens, G.; Baeyens-Bolant, D.; Delaunois, G.; Vinh, L.; Piret, W.; David, C. *Eur. Polym. J.* **1978**, *14*, 291.
(30) (a) Grassie, N.; Weir, N. A. *J. Appl. Polym. Sci.* **1965**, *9*, 975. (b) Kouvacevic, V.; Bravar, M.; Hace, D. *Angew. Makromol. Chem.* **1985**, *137*, 175. (c) Beachell, H. C., Smiley, H. *J. Polym.* Sci., **1967**, *5*, 1635. (d) Lucki, J.; Ranbpy, B. *Polym. Degrd. and Stability*, **1979**, *1*, 251.

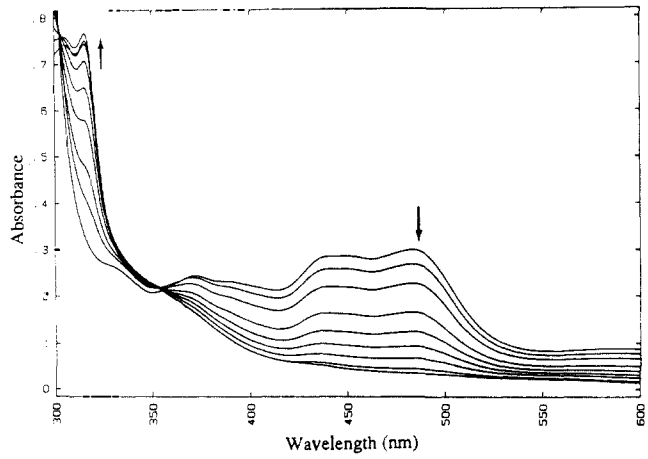

Figure 2. Visible absorption spectral changes in CH_3CN showing sequential oxidation of $[PS\text{-}Os^{II}_{30}](PF_6)_{60}$ (2.4×10^{-5}) by Ce^{IV}, b = 1 cm. The loss in absorbance in the visible region is proportional to the amount of Ce^{IV} added.

fectively catalyze the photooxidation of various carbinols to aldehydes by visible light.[31]

Because of the reactivity of the Ru^{III}-containing polymers, our efforts were focused on $[PS\text{-}Os^{II}_{30}](PF_6)_{60}$ because Os^{III} is a less potent oxidant than Ru^{III}. Addition of Ce^{IV} to $[Ps\text{-}Os^{II}_{30}](PF_6)_{60}$ in CH_3CN was utilized to achieve controlled compositions of Os^{II} and Os^{III} on the polymeric backbone without complications from self-oxidation. The analysis of content with regard to oxidation state was accomplished by monitoring the decrease in absorbance in the MLCT region, λ_{max} at 460 nm (ϵ = 12 400 cm^{-1} M^{-1}). Figure 2 illustrates the spectral changes that occur in solutions containing $[PS\text{-}Os_{30}](PF_6)_{60}$ with added Ce^{IV}. For quantitative spectrophotometric titrations with Ce^{IV}, the reaction stoichiometry was established to involve 1 equiv of Ce^{IV} per equiv of Os^{II}. The stepwise oxidation was also minitored by observing the relative decrease in integrated emission intensities or the integrated areas under lifetime decay curves as a function of added Ce^{IV}. The Os^{III} sites are nonemissive.

If it is assumed that the efficiency of emission of each Os^{II} site is unaffected by the Os^{III}/Os^{II} ratio, the decrease in integrated emission efficiency with added Ce^{IV} is given in eq 8. In eq 8 the

$$\frac{I}{I_0} = \left(\frac{[Os^{II}]}{[Os^{II}]_{tot}}\right)\phi = \left(1 - \frac{[Ce^{IV}]}{[Os^{II}]_{tot}}\right)\phi \qquad (8)$$

quantity I is the integrated emission intensity from $[PS\text{-}Os^{III}_{n}Os^{II}_{(30-n)}]^{(60+n)+}$, I_0 is the integrated intensity from unoxidized $[PS\text{-}Os^{II}_{30}]^{60+}$, and ϕ is the emission quantum yield for $[PS\text{-}Os^{II}_{30}]^{60+}$. The derivation of this equation assumes optically dilute solutions where $(1 - 10^{-\epsilon bc}) \simeq 2.3\epsilon bc$. It also assumes that $[Os^{II}] = [Os^{II}]_{tot} - [Os^{III}] = [Os^{II}]_{tot} - [Ce^{IV}]$ where $[Os^{II}]_{tot}$ is the total concentration of initial Os^{II} sites.

In Figure 3a is shown a plot of I/I_0 vs $([Ce^{IV}]/[Os^{II}]_{tot})$ and of a least-squares fit to the data of the form $y = -1.04x + 1.02$. From the fact that the slope and intercept are of near unit magnitude, it can be inferred that the emission quantum yield for Os^{II*} is little affected by oxidation of adjacent sites to Os^{III}.

In Figure 3b is shown a plot of excited-state lifetime as a function of the mole fraction of Os^{III} in the polymer. The plot shows that the Os^{II*} lifetime of 46 ns is unaffected by the presence or even the number of adjacent Os^{III} sites. The scatter of ±1.5 ns in the lifetimes is within experimental error.

There are subtleties in the lifetime data. In Figure 4 are shown ln (intensity) vs time plots for three polymers having different $Os^{III/II}$ ratios. In the polymers $[PS\text{-}Ru^{II}_{30}](PF_6)_{60}$ and $[PS\text{-}Os^{II}_{30}](PF_6)_{60}$, which are completely loaded in M^{II}, multiphoton excitation gives rise to complex decay kinetics at early times in the decay profile.[32] The lifetimes cited in Figure 3 were determined by analyzing the decays after one lifetime had occurred in order to avoid such effects. As the Os^{II} sites were diluted by Os^{III}, the emission decay data more nearly followed simple, single-exponential kinetics. The decay kinetics became exponential when the extent of oxidation of Os^{II}/Os^{III} was >50%. These observations suggest that dilution of Os^{II} by Os^{III} *suppresses* the multiphoton effects.

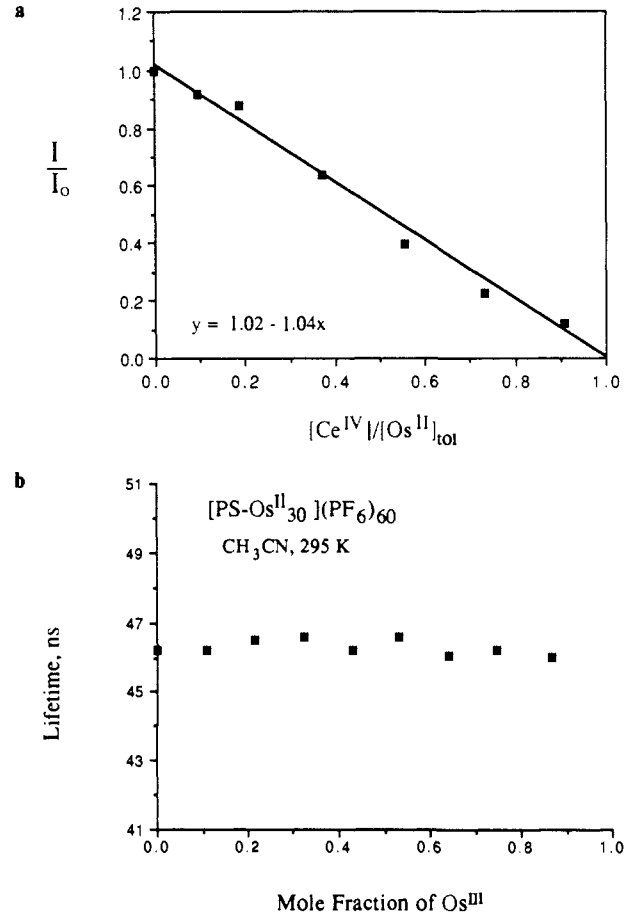

Figure 3. Plots of (a) I/I_0 vs $[Ce^{IV}]/[Os^{II}]_{tot}$ (see text) for $[PS\text{-}Os^{II}_{30}](PF_6)_{60}$ in CH_3CN. The quantities I_0 and I are the integrated emission intensities without and with added Ce^{IV}; $[Os^{II}]_{tot}$ is the total concentration of Os^{II} sites. The slope and intercept of the least squares line are −1.04 ± 0.01 and 1.02 ± 0.02, respectively. Plot of (b) excited-state lifetimes of $[PS\text{-}Os^{III}_{x}Os^{II}_{30-x}]^{(60+x)}$ vs mole fraction of Os^{III} in CH_3CN at 295 K.

Excited-State Electron-Transfer Quenching. With either $[PS\text{-}Os^{II}_{30}](PF_6)_{60}$ or $[PS\text{-}Ru^{II}_{30}](PF_6)_{60}$ it is possible to build up multiple redox equivalents photochemically. In Figure 5 is shown a plot of integrated emission intensity versus photolysis time for $[PS\text{-}Os^{II}_{30}]^{60+}$ with an added, excess amount of the irreversible oxidative quencher, $4\text{-}CH_3OC_6H_4N_2^+$ (ArN_2^+).[33] The quenching reactions are shown in eq 9.

$$[PS\text{-}Os^{II}_{30}]^{60+} \xrightarrow{h\nu} [PS\text{-}Os^{II*}Os^{II}_{29}]^{60+}$$

$$[PS\text{-}Os^{II*}Os^{II}_{29}]^{60+} + ArN_2^+ \rightarrow [PS\text{-}Os^{III}Os^{II}_{29}]^{61+} + ArN_2^{\circ} \qquad (9)$$

$$(ArN_2^{\circ} \xrightarrow{CH_3CN} Ar\text{-}H + N_2)$$

$$\cdots$$

$$\cdots$$

$$\cdots$$

$$[PS\text{-}Os^{III}_{29}Os^{II}]^{89+} + ArN_2^+ \xrightarrow{h\nu} [PS\text{-}Os^{III}_{30}]^{90+} + ArN_2^{\circ}$$

(31) Yelo-Cano, H.; Deronizier, A. *Tetrahedron Lett.* **1984**, *25*, 5517.

(32) Worl, L. A.; Danielson, E.; Strouse, G. F.; Murtaza, Z.; Meyer, T. J. Manuscript in preparation.

(33) Cano-Yelo, H.; Deronzier, A. *Faraday Trans. I* **1984**, 3011.

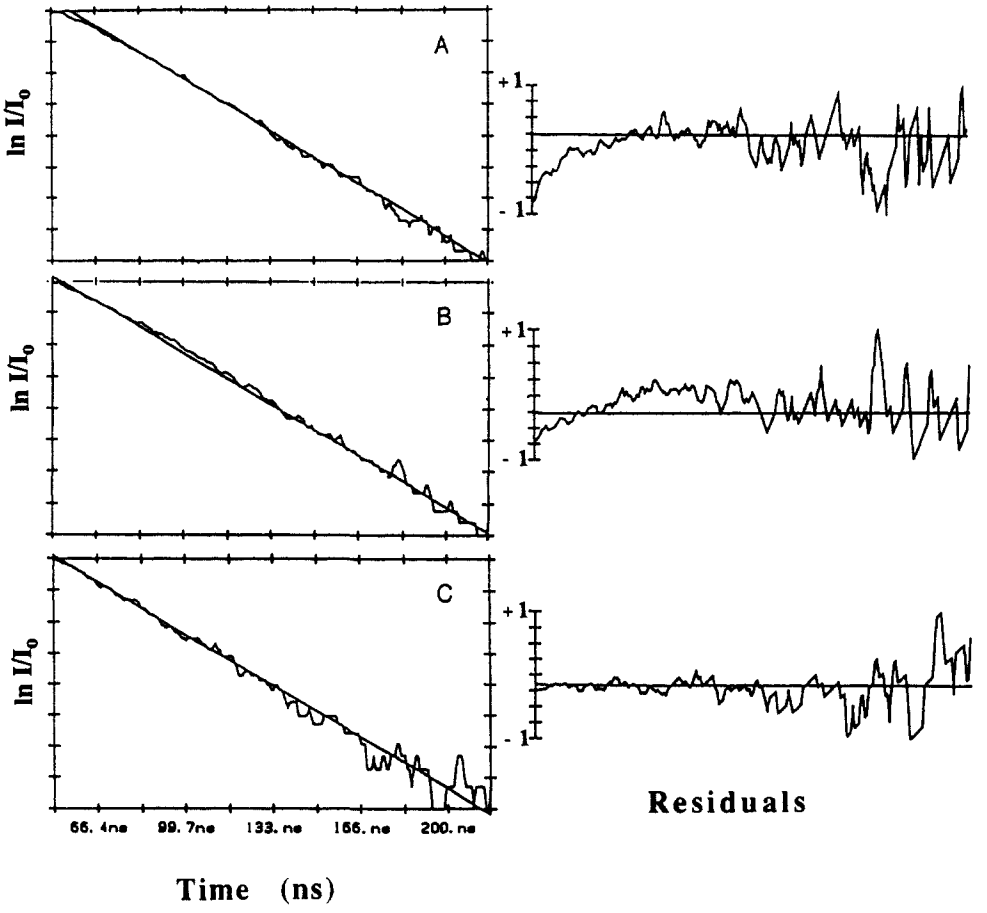

Figure 4. Plot of ln (I/I_0) vs time and of the deviation from first-order behavior in the residual plots to the right for the emission-decay profiles of (A) $[PS\text{-}Os^{II}_{30}]^{60+}$, (B) $[PS\text{-}Os^{III}_{6}Os^{II}_{24}]^{66+}$, and (C) $[PS\text{-}Os^{III}_{21}Os^{II}_{9}]^{81+}$ in CH_3CN. The lines are least-squares fits to the equation $I(t) = A\exp(-kt)$. The plots of the residuals provide a measure of the quality of the fits.

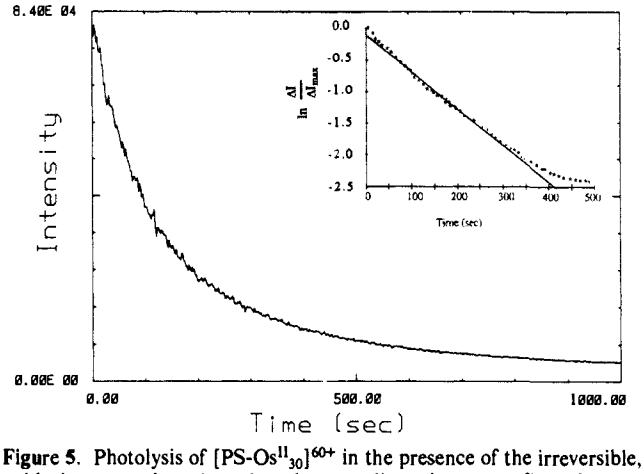

Figure 5. Photolysis of $[PS\text{-}Os^{II}_{30}]^{60+}$ in the presence of the irreversible, oxidative quencher 4-methoxybenzenediazonium tetrafluoroborate, $([ArN_2](BF_4)$, $3.8 \times 10^{-3})$, in 1.0 M $[N(n\text{-}C_4H_9)_4](PF_6)$-$CH_3CN$ at 295 ± 2 K. The decrease in emission intensity at 770 nm that accompanies 460-nm photolysis in the presence of 0.02 M of the quencher is shown. The line is the result of a linear least-squares fit assuming first-order behavior, where ΔI is the emission intensity and ΔI_{max} the intensity at time 0. The slope and intercept of the least-squares line shown in the insert were -5.9×10^{-3} s^{-1} and −0.1, respectively.

In electrochemical studies, a single, broad $Os^{III/II}$ wave appeared in cyclic voltammograms of $[PS\text{-}Os^{II}_{30}]^{60+}$ at $E_{1/2} = 0.75$ V vs the saturated sodium calomel electrode (SSCE) at a scan rate of 100 mV/s. The peak-to-peak separation under these conditions was 110 mV. Potentials for the separate $Os^{III/II}$ couples, e.g., $[PS\text{-}Os^{III}Os^{II}_{29}]^{61+}/[PS\text{-}Os^{II}_{30}]^{60+}$ or $[PS\text{-}Os^{III}_{10}Os^{II}_{20}]^{70+}/[PS\text{-}Os^{III}_{9}Os^{II}_{21}]^{69+}$, were not resolved in the voltammograms. From the electrochemical data, it can be inferred that the potentials for the series of couples that interrelate $[PS\text{-}Os^{II}_{30}]^{60+}$ and $[PS\text{-}Os^{III}_{30}]^{90+}$ are completely overlapped. This means that partial oxidation to an intermediate stage, for example to $[PS\text{-}Os^{III}_{10}Os^{II}_{20}]^{70+}$, necessarily gives a *distribution* of oxidation state compositions in solution.[34] The chemical formula only conveys the fact that the distribution has an *average* Os^{III} content of 10 per strand.

Although the oxidized ruthenium polymer could be generated photochemically, it spontaneously reverted to Ru^{II} as discussed above. The fully oxidized Os polymer, $[PS\text{-}Os^{III}_{30}]^{90+}$, was stable for ~2 h after generation. The emission quantum yields before and after photolysis for 1000 s were 0.0064 and 0.0002, respectively, a decrease to 3% of the original intensity.

The decay of the emission intensity with the extent of photochemical oxidation followed nearly first order behavior for ~60% of the reaction (insert, Figure 5). A simple, first-order loss in emission intensity is predicted for the limiting case where there is a single quenching rate constant (k_q) and lifetime (τ) for Os^{II*} regardless of the extent of photochemical oxidation (Appendix). In this limit, the slope of the first-order plot is related to the incident light intensity (I_0), the quenching rate constant (k_q), and the quencher concentration at low light absorbance by eq 10 (Appendix). In eq 10, b is the path length and ϵ the molar extinction coefficient at the excitation wavelength (460 nm). By

$$\text{slope} = -2.303 I_0 b\epsilon\left[\frac{k_q[Q]}{k_q[Q] + 1/\tau}\right] = -2.303 I_0 b\epsilon\phi_q \qquad (10)$$

using eq 10 and the experimental slope of -5.92×10^{-3} s^{-1} (Figure

(34) (a) Flanagan, J. B.; Margel, S.; Bard, A. C; Anson, F. C. *J. Am. Chem. Soc.* **1978**, *100*, 4248. (b) Brown, G. M.; Callahan, R. W.; Johnson, E. C.; Meyer, T. J.; Weaver, T. R. *Am. Chem. Symp. Ser.* **1975**, *No. 5*, 66. (c) Brown, G. M.; Meyer, T. J.; Cowan, D. O.; LaVanda, C.; Kaufman, F.; Roling, P. V.; Rausch, M. D. *Inorg. Chem.* **1975**, *14*, 506.

5, inset, $b = 1.00$ cm, $\epsilon = 12400$ M^{-1} cm^{-1}), $\phi_q = 0.12$ at $[ArN_2^+] = 3.8 \times 10^{-3}$ M. At this concentration and with $\tau = 46$ ns, $k_q = 7.6 \pm 1.0 \times 10^8$ M^{-1} s^{-1}. This value is in good agreement with $k_q = 1.3 \pm 0.2 \times 10^9$ M^{-1} s^{-1}, which was measured by Stern–Volmer lifetime quenching of emission from $[PS\text{-}Os^{III}{}_{12}Os^{II}{}_{18}]^{72+}$. A solution containing the mixed-valence polymer was prepared by partial oxidation of $[PS\text{-}Os^{II}{}_{30}]^{60+}$ by using Ce^{IV}. The quenching kinetics for these polymers are, in general, complicated by multiphoton effects. They are currently under investigation with a variety of quenchers.[32]

Discussion

The Accumulation of Multiple Redox Equivalents on Single Polymeric Strands. The experiments described here demonstrte that it is possible to build up multiple redox equivalents on individual polymeric strands by a series of single electron transfer quenching events. With the irreversible, oxidative quencher, 4-methoxybenzenediazonium cation, sequential excitation and quenching led to the stepwise buildup of 30 oxidative equivalents (eq 9). Only a small fraction of unquenched emission remained after a photolysis period of 1000 s (Figure 5).

From the results of the quenching study in Figure 5, the rate of Os^{II}* quenching is relatively unaffected over the course of the reaction as Os^{II} is converted into Os^{III}. The slight curvature in the first-order plot shows that k_q decreases as the reaction proceeds. This is probably an electrostatic effect since the quencher is cationic and the charge on the polymer increases during the course of the photolysis.

The key to the buildup and storage of multiple redox equivalents is the absence of appreciable quenching of M^{II}* by M^{III}. This is demonstrated for the mixed-valence polymer by the independence of the lifetime and emission quantum yields (Figure 3) on Os^{III} content. In fact, as suggested by the lifetime data in Figure 3b, *the M^{III} site can act as a diluent of Os^{II}* thus diminishing the effect of multiphoton excitation.

The absence of intramolecular quenching cannot be attributed to spatial isolation of the sites. The complexes are large, ~14 Å in diameter, and the polymer repeat length is small (5–7 Å, depending on tacticity). From the results of molecular modeling study, the polymer morphology appears to be an extended, relatively tight helix with the electrostatic repulsion between the 2+ charged sites dominating the overall structure. In these calculations the simplifying assumptions were made that the initial *p*-chloromethyl sites were purely para and the polymer isotactic.[32,35] The combination of electrostatic repulsions between M^{2+} sites, and the constraints imposed by the natural bond lengths and angles of the hydrocarbon backbone tend to distribute the chromophores into domains of local, nearly tetrahedral symmetry with an average M^{II}–M^{II} interpair separation distance of 18.2 ± 0.8 Å. The average separation between the van der Waals distances at the peripheries of adjacent metal sites was ~4 Å. The molecular model shows that relatively small rotation motions can promote close contact between adjacent chromophores.[32,35]

Intramolecular processes involving metal complex sites in related polymers are known to be rapid. In a mixed Ru^{II}–anthryl polymer based on the same backbone and the same linkage chemistry, energy transfer quenching of Ru^{II}* by the anthryls is known to be rapid.[36]

The reactions of eq 6 involving intramolecular electron or energy transfer provide pathways for bringing to adjacent sites the Os^{II} excited state and the Os^{III} quencher. Regardless of whether or not these pathways compete with excited-state decay, it is clear from the experimental data that intramolecular quenching by Os^{III} or Ru^{III} does not compete with the spontaneous decay of Os^{II}* or Ru^{II}* in the mixed-valence polymers. Even in polymers where, on the average, Os^{II}* must have a nearest neighbor Os^{III}, there is no evidence for oxidative quenching.

The Os^{II}* excited states have access to the usual radiative and nonradiative decay channels that are available to MLCT excited states, and it is these channels that dominate loss of the excited states.[22,37] From the unperturbed lifetimes in the mixed-valence polymers, and their associated uncertainties, we estimate that $k < 2 \times 10^6$ s^{-1} for intramolecular quenching (eq 11).

Slow intramolecular quenching is a consequence of the restrictions imposed on electron transfer in the "inverted region". The free energy change for intramolecular quenching (eq 11) is −1.6 eV. This energy release is the same as the energy release

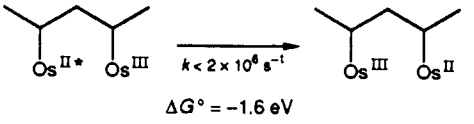

$\Delta G° = -1.6$ eV (11)

that occurs upon nonradiative decay of Os^{II}* (eq 12). The products are the same in either case, but the local oxidation state distribution is reversed.

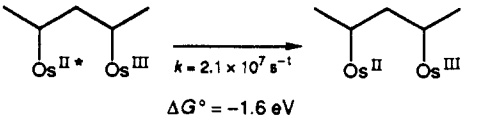

$\Delta G° = -1.6$ eV (12)

The dynamics of the quenching process depend upon (1) vibrational overlaps between the initial and final states for participating normal modes at *both* the Os^{II}* and Os^{III} sites, (2) solvent librations in the vicinity of both sites, and (3) electronic coupling by weak outer-sphere interactions. In nonradiative decay, the release of the initial electronic energy occurs into the vibrational and librational modes at a single site. There is electron transfer only in the sense that there is a change in radial electronic distribution between the excited and ground states. The electronic coupling between states is vibronic in character and utilizes so-called promoting modes.[18]

Because intramolecular quenching is slow relative to excited-state decay, it is possible to build up multiple redox equivalents on the individual strands of the Ru^{II} and Os^{II} polymers. The multielectron transfer character of these systems may have significance in future experiments in providing a means for coupling single-electron events to the multielectron requirements of small molecule reactions. The next achievement will lie in combining the multielectron capabilities of the polymers with known catalytic sites for small-molecule reactions.

Acknowledgments are made to the Department of Energy under grant No. DE-FG05-86ER13633 and to the National Institute of Health for postdoctoral support (S. Baxter) under grant No. GM13382-01 for support of this research.

Appendix

The rate of loss of Os^{II}* by oxidative quenching by quencher Q is given by eq A1.[38] In eq A1, η is the efficiency of formation

$$-[Os^{II}]/dt = I_a \eta \phi_q \quad \text{(A1)}$$

of the emitting state following excitation. It is 1 for $[Ru(bpy)_3]^{2+}$*.[39] The quantity I_a is the intensity of light absorbed by Os^{II} per unit volume. It is given by eq A2. In eq A2, I_0 is

$$I_a = I_0(1 - 10^{-\epsilon b[Os(II)]}) \sim 2.303 I_0 \epsilon b [Os^{II}] \quad \text{(A2)}$$

the intensity of incident light per unit volume in mol/s·dm³, ϵ is the molar extinction coefficient of Os^{II} at the irradiation wavelength in M^{-1} cm^{-1}, and b is the path length in cm. In eq A2,

(35) Commercial versions of Sybyl/Mendyl/Nitro software were used in the modeling studies in conjunction with our own program for electrostatic minimization.

(36) Strouse, G. F.; Worl, L. A.; Younathan, J. N.; Meyer, T. J. *J. Am. Chem. Soc.* **1989**, *111*, 9101.

(37) Meyer, T. J. *Pure Appl. Chem.* **1986**, *58*, 1193.

(38) See for example: Calvert, J. G.; Pitts, J. N. *Photochemistry*; John Wiley & Sons, Inc.: New York, 1966; Chapter 6. Ferraudi, G. J. *Elements of Inorganic Photochemistry*; John Wiley & Sons: New York, 1988.

(39) (a) Demas, J. N.; Taylor, D. G. *Inorg. Chem.* **1979**, *18*, 3177. (b) Bolletta, F.; Juris, A.; Maestri, M.; Sandrini, D. *Inorg. Chim. Acta* **1980**, *44*, L175.

it is assumed that Os^{II} is the only appreciable light absorber at 460 nm. The approximation in eq A2 is valid for optically dilute solutions.

The quenching quantum yield is given by eq A3. In eq A3,

$$\phi_q = \left[\frac{k_q[Q]}{k_q[Q] + 1/\tau}\right] \quad \text{(A3)}$$

k_q is the quenching rate constant for quencher Q and τ is the lifetime with no added quencher. Incorporating the relationships in eqs A2 and A3 into eq A1 and integrating from time = 0 to t gives eq A4. Substitution of the relationships $[Os^{II}*]_t = C(I_t - I_\infty)$ and $[Os^{II}*]_{t=0} = C(I_0 - I_\infty)$ into eq A4 provides the basis

$$\ln\left[\frac{[Os^{II}]_t}{[Os^{II}]_{t=0}}\right] = -kt = -2.303 I_0 \epsilon b \phi_q t = -2.303 I_0 \epsilon b \left[\frac{k_q[Q]}{k_q[Q] + 1/\tau}\right] t \quad \text{(A4)}$$

for the plot in Figure 5 and leads to the expression for the slope in eq 10. In eq A4, I_0, I_t, and I_∞ are the emitted light intensities at times 0, t, and ∞, and C is a constant.

Synthesis of Octamethylferrocene Derivatives via Reaction of (Octamethylferrocenyl)methyl Carbocation with Nucleophiles and Application to Functionalization of Surfaces

Chaofeng Zou and Mark S. Wrighton*

Contribution from the Department of Chemistry, Massachusetts Institute of Technology, Cambridge, Massachusetts 02139. *Received January 31, 1990*

Abstract: Formylation of octamethylferrocene, $Fe(C_5Me_4H)_2$, using *N,N'*-dimethylformamide/$OPCl_3$ in $CHCl_3$ solvent at 60–70 °C gives octamethylformylferrocene in high yield (~95%). The aldehyde can be converted to a CN group to give octamethylcyanoferrocene or can be used to prepare ethyl β-(octamethylferrocenyl)acrylate. Most important, reductionn of octamethylformylferrocene using $LiAlH_4$ in Et_2O yields the alcohol in ~95% yield. Acid-catalyzed (HBF_4) dehydration of the alcohol, III, leads to formation of (octamethylferrocenyl)methyl carbocation in almost quantitative yield. The carbocation I can be isolated as an orange-red BF_4^- salt in ~90% yield from octamethylferrocene. I shows sharp ^{13}C and ^1H NMR spectral features consistent with formulation as a diamagnetic Fe(II) species with the positive charge localized on the C having two H's. I slowly dimerizes, even in the solid state, to a C–C coupled product with two Fe(III) centers. The paramagnetic, blue-green dimer can be reduced with cobaltocene or aqueous $Na_2S_2O_4$ to 1,2-bis(octamethylferrocenyl)ethane. Reaction of (octamethylferrocenyl)methyl carbocation with nucleophiles is a convenient synthetic route to octamethylferrocene derivatives, which have proved difficult to obtain by electrophilic substitution of octamethylferrocene. Reaction of the new carbocation I has been used to synthesize octamethylferrocenyl derivatives in good to excellent yields (~60–95%) via reaction with amines, thiols, or CN^-. Reaction of (octamethylferrocenyl)methyl carbocation with surface-confined nucleophiles such as NH_2 or SH [surfaces derivatized with $(MeO)_3Si(CH_2)_3NH_2$ or $(MeO)_3Si(CH_2)_3SH$] is a convenient way to attach octamethylferrocene derivatives to surfaces including SiO_2, Pt, and indium tin oxide (ITO).

We report the synthesis of octamethylferrocene derivatives via nucleophilic attack on the carbocation represented by I, eq 1, and

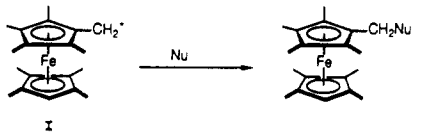

(1)

I

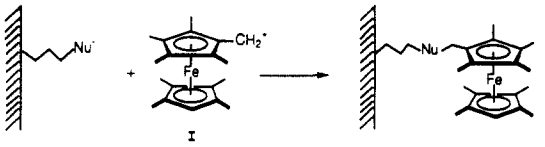

(2)

I

the reaction of I with surface-confined nucleophiles, eq 2. The synthesis, structure, and reactivity of a variety of ferrocene derivatives has been well documented over the past 30 years,[1] including detailed studies of ferrocenylmethyl carbocations.[2] However, polymethylferrocene derivatives having transformable functional groups have been relatively unexplored.

We are interested in using polymethylferrocene reagents as electrode surface modifiers. The chemistry represented by eq 2 is a new way to derivatize surfaces with a durable, redox-active molecule that may be of importance in electrocatalysis.[3] For example, it has demonstrated that electrode surfaces derivatized with a pentamethylferrocene derivative give a nearly reversible response to cytochrome *c*.[3f] For mediated oxidation and reduction of cytochrome *c* the potential of ferrocene itself is far too positive to be a reversible mediator. More recently we have used a ferrocene group as a labeling "tag" to study the surface coordination

(1) (a) Marr, G.; Rockett, B. W. *J. Organomet. Chem.* **1988**, *343*, 79, and the annual survey of the previous years. (b) Perevalova, E. G.; Nikitina, T. V. In *Organometallic Reactions*; Becker, E. I., Tsutsui, M., Eds.; Wiley: New York, 1972; Vol. 4, p 163. (c) Bublitz, D. E.; Rinehart, K. L., Jr. *Org. React.* **1969**, *17*, 1. (d) Rosenblum, M. In *Chemistry of the Iron Group Metallocenes*: Seyferth, D., Ed.; Interscience Publishers: New York, 1965.

(2) (a) Watts, W. E. *J. Organomet. Chem. Libr.* **1979**, *1*, 399–459. (b) Kreindlin, A. Z.; Fadeeva, S. S.; Rybinskaya, M. I. *Izv. Akad. Nauk. SSSR, Ser. Khim.* **1983**, *2*, 403.

(3) (a) Wrighton, M. S.; Palazzotto, M. C.; Bocarsly, A. B.; Bolts, J. M.; Fischer, A. B.; Nadjo, L. *J. Am. Chem. Soc.* **1978**, *100*, 7264. (b) Wrighton, M. S.; Austin, R. G.; Bocarsly, A. B.; Bolts, J. M.; Haas, O.; Legg, K. D.; Nadjo, L.; Palazzotto, M. C. *J. Electroanal. Chem. Interfacial Electrochem.* **1978**, *87*, 429. (c) Bolts, J. M.; Bocarsly, A. B.; Palazzotto, M. C.; Walton, E. G.; Lewis, N. S.; Wrighton, M. S. *J. Am. Chem. Soc.* **1979**, *101*, 1378. (d) Bolts, J. M.; Wrighton, M. S. *J. Am. Chem. Soc.* **1979**, *101*, 6179. (e) Fischer, A. B.; Bruce, J. A.; McKay, D. R.; Maciel, G. E.; Wrighton, M. S. *Inorg. Chem.* **1982**, *21*, 1766. (f) Chao, S.; Robbins, J. L.; Wrighton, M. S. *J. Am. Chem. Soc.* **1983**, *105*, 181.

0002-7863/90/1512-7578$02.50/0